

***In silico* ADMET and molecular docking study on searching potential inhibitors from limonoids and triterpenoids for COVID-19**

Seshu Vardhan and Suban K Sahoo*

Department of Applied Chemistry, S.V. National Institute of Technology (SVNIT), Surat-395007, India. (E-mail: sks@chem.svnit.ac.in)

Abstract

The computational strategies like molecular docking, simulation, *in silico* ADMET and drug-likeness prediction were adopted to search potential compounds that can inhibit the effects of SARS-CoV-2. Considering the published literatures on medicinal importance, total 154 phytochemicals with analogous structure from limonoids and triterpenoids were selected to search potential inhibitors for the five protein targets of SARS-CoV-2, i.e., 3CLpro (main protease), PLpro (papain like protease), SGp-RBD (spike glycoprotein-receptor binding domain), RdRp (RNA dependent RNA polymerase, ACE2 (angiotensin converting enzyme 2). Analyses of the *in silico* computational results and reported medicinal uses, the phytochemicals such as 7-deacetyl-7-benzoylgedunin, epoxyazadiradione, limonin, maslinic acid, glycyrrhizic acid and ursolic acid were found to be effective against the target proteins of SARS-CoV-2. The protein-ligand interaction study revealed that these phytochemicals bind at the main active site of the target proteins. Therefore, the core structure of these potential hits can be used for further lead optimization to design drugs for SARS-CoV-2. Also, the plants extracts like neem, tulsi, citrus and olives containing these phytochemicals can be used to formulate suitable therapeutics approaches in traditional medicines.

Keywords: Coronavirus; COVID-19; Molecular docking; ADMET, Limonoids, Triterpenoids.

1. Introduction

The ongoing research focused globally to formulate suitable therapeutic approaches to control the effects of the severe acute respiratory syndrome coronavirus 2 (SARS-CoV-2) to human life that caused the disease COVID-19. The first patient infected with SARS-CoV-2 was detected in December, 2019 at Wuhan, China. Subsequently, the virus spread across 187 countries and territories due to its high human to human contagious nature and infected 4006,257 as of 11th May 2020 with a total death of 278,892 [1]. The uncontrolled spread pushed the World Health Organization (WHO) to declare the outbreak of SARS-CoV-2 as a public health emergency of international concern (PHEIC) on 30th Jan 2020, whereas a pandemic on 11th March 2020 [2]. Effective steps like identification of infected persons through rapid diagnosis, and quarantined them to stop further spread of the virus are underway to fight against this pandemic. However, the non-availability of medically proven efficacious drugs or vaccines is the main concern of COVID-19 pandemic [3]. Repurpose of some approved drugs like hydroxychloroquine, remdesivir, favipiravir, arbidol, hydroxychloroquine/azithromycin, lopinavir/ritonavir and lopinavir/ritonavir combined with interferon beta etc. are used, but despite some promising results further clinical results are required to examine their mechanisms of inhibition, efficacy and safety in the treatment of COVID-19 [4-8]. Therefore, both computational and experimental approaches are adopted to search suitable drugs from the library of FDI-approved drugs and also drugs under clinical trial but not yet approved to repurpose against the COVID-19. Simultaneously, the recent reports supporting the use of traditional medicines as adjuvant for treating COVID-19 [9-11] and therefore, efforts are also going to integrate the use of both western drugs and traditional medicines to formulate suitable therapeutic strategies.

The computational approaches like dynamic simulations, molecular docking, drugs likeness prediction, *in silico* ADMET study etc. are valuable tools to screen potential drugs/molecules from various databases that contained in lakhs. The computational screening save both experimental cost and time in the field of drugs discovery. Considering the recent results of the use of traditional medicines in managing the epidemic of COVID-19 [9-11], our ongoing research is focused on to screen phytochemicals found mainly in the Indian medicinal plants with the important objectives: (i) to search phytochemicals that bind effectively at the active sites of the protein targets of SARC-VoV-2, (ii) to propose important hits that can be further investigated for lead optimization and drugs discovery, and (iii) to provide computational evidences for formulating Indian traditional medicines in controlling the spread and effects of SARC-VoV-2. Our literatures survey revealed that the triterpenoids like 3 β -friedelanol from *Euphorbia neriifolia*, quinone-methide triterpenoids extracted from *Tripterygium regelii* (Celastraceae) and glycyrrhizin from *Glycyrrhiza glabra* are experimentally proven to inhibit the effects of SARS-CoV (first identified in Guangdong, China in 2002) [12-15]. Also, our recent molecular docking studies of phytochemicals against the protein targets of SARS-CoV-2 supported the higher binding affinity towards limonin, a triterpenoid found in citrus [16].

Considering the above facts, we selected 154 phytochemicals from limonoids and triterpenoids by considering their basic knowledge on medicinal importance and structural analogous to search potential hits for the five protein targets of SARS-CoV-2 i.e., 3CLpro (main protease), PLpro (papain like protease), SGp-RBD (spike glycoprotein-receptor binding domain), RdRp (RNA dependent RNA polymerase, ACE2 (angiotensin converting enzyme 2). The computational approaches like *in silico* ADMET, drugs likeness, simulations and molecular docking studies were performed to propose the potential hits from the 154 phytochemicals.

2. Experimental

2.1. Compounds and proteins selection

The selected 154 biologically important compounds from limonoids and triterpenoids were collected from various sources and screened to filter potential compounds that can inhibit the activity of SARS CoV-2. The SDF files of the selected phytochemicals were retrieved from EMBL-EBI (www.ebi.ac.uk/chebi/advancedSearchFT.do) and PUBCHEM (<https://pubchem.ncbi.nlm.nih.gov/>). The collected structures of the phytochemicals were further optimized by semi-empirical PM6 method coded in the computational program Gaussian 09W [17]. The optimized structures were converted to PDB file format by using the program GaussView 5.0. The crystallography structures of the SARS-CoV-2 protein targets (3CLpro, PDB ID: 6LU7; PLpro, PDB ID: 4MM3; RdRp, PDB ID: 6M71; SGp-RDB, PDB ID: 2ghv; ACE2, PDB ID: 6M17) were retrieved from the PDB database (www.rcsb.org).

2.2. Molecular docking and simulations

The molecular docking studies were carried out by using Autodock Vina1.1.2 [18], and the binding energies of the limonoids and triterpenoids were estimated towards SARS-CoV-2 therapeutic targets. The proteins 3D structures retrieved from RCSB PDB databases, and some of the missing residues of the proteins were modelled using Swiss model online tools to generate the fine structures. The refined protein structures were analysed using the Ramachandran plot. Different conformations, hydrophobic sites are identified and analysed using BIOVIA Discovery studio visualization tool.

The protein structure flexibility and dynamics simulations were performed using CABSflex2.0 online simulation tool with the default options [19]. The simulated model generated through trajectory clustering k-medoid method. This tool calculates the protein dynamic simulations at 10 ns, predicts fluctuations and protein aggregation propensity.

2.3. ADMET and drug-likeness prediction

After the molecular docking analysis of 154 compounds with the five protein targets of SARS-CoV-2, the absorption, distribution, metabolism, elimination and toxicity (ADMET) of the 47 best dock scored limonoids and triterpenoids were further screened using online tool '<http://biosig.unimelb.edu.au/pkcsmprediction>' to predict their important pharmacokinetic properties. ADMET properties include absorption: Caco-2 permeability, water solubility, human intestinal absorption, P-glycoprotein substrate, P-glycoprotein I and II inhibitors, skin permeability; Distribution: VDss (Volume of Distribution), Fraction unbound, Blood brain barrier (BBB) permeability, CNS permeability; Metabolism: Cytochrome P450 inhibitors, CYP2D6/CYP3A4 substrate; Excretion: renal OCT2 substrate, Drug total clearance. Toxicity: Rat LD50, AMES toxicity, T. pyriformis toxicity, Minnow toxicity, maximum tolerated dose, oral rat chronic toxicity, Hepatotoxicity, skin sensitization, hERG I and II inhibitors [20].

Drug-likeness properties were predicted using the online tool molinspiration (<https://www.molinspiration.com/cgi-bin/properties>). Providing SMILES inputs of selected compounds into the tool calculated the LogP values to predict the molecular properties and bioavailability scores resulting in the drug likeness of the compound. Based on drug likeness and bioavailability capabilities, the potential compounds were finalized for further study. The calculations of LogP are based on the formula satisfying lipophilicity, hydrophobicity and polarity of the compound explains the ability of molecules that could bind to hydrophobic sites of target proteins [21].

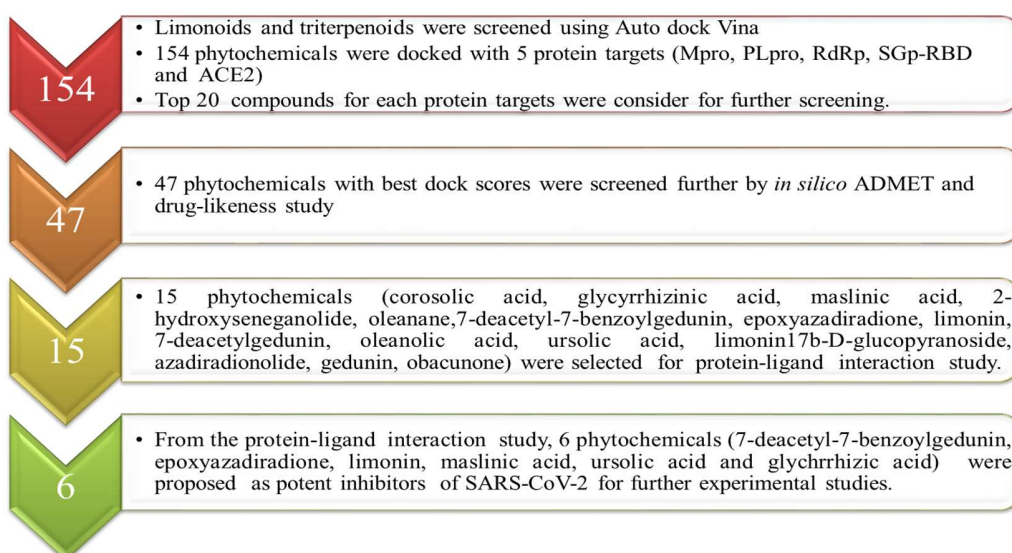
$$\text{Lipophilicity} = \text{Hydrophobicity} - \text{Polarity}$$

$$\text{Log P} = aV + \Lambda \quad (V=\text{Molecular Volume}, \Lambda=\text{Polarity term})$$

3. Results and discussion

3.1. Selection of the phytochemicals

Our recent molecular docking study on searching inhibitors for COVID-19 revealed that the phytochemicals limonin known for inhibiting the replication of retroviruses like HTLV-I and HIV-1 showed the higher dock score towards the three protein targets (spike glycoprotein, RdRp and ACE2) of SARS-CoV-2, and comparatively higher than the drug hydroxychloroquine [21]. Limonin, the highly oxygenated triterpenoid dilactone is the first isolated limonoids and till date more than 300 limonoids are isolated and characterized. The plants containing limonoids including the structural analogous triterpenoids, such as citrus, neem, basils and licorice etc., are reported for various pharmaceutical properties like antiviral, antifungal, antibacterial, anticancer and antimalarial, and also used routinely in the Indian traditional medicine (ayurveda) to treat various health problems. Therefore, a basic preliminary screening of phytochemicals from limonoids and triterpenoids were carried out based on the published literatures, and total 154 phytochemicals were selected, and then studied against the five protein targets (3CLpro, PLpro, spike glycoprotein, RdRp and ACE2) of SARS-CoV-2 (**Scheme 1**).



Scheme 1. Flow-chart showing the steps to screen phytochemicals for the COVID-19.

3.2. Molecular docking results

The selected 154 phytochemicals were screened against the five important protein targets, i.e., Mpro or 3CLpro, PLpro, SGp-RBD, RdRp and ACE2 of SARS-CoV-2 by performing molecular docking analysis using the Autodock Vina computational program. The structural spike glycoprotein (S protein) of SARS-CoV-2 recognizes with the transmembrane protein of host cell receptor ACE2 [22,23]. This also internalizes the virus into the endosomes where the conformational changes take place in the spike glycoprotein. It acts as a viral fusion peptide that covers up S2 cleavage that occurs during virus endocytosis. Thereafter, RdRp facilitates the viral genome replication [24]. The main protease 3CLpro and PLpro act as proteases in the process of proteolysis of viral polyprotein into functional units [25]. In short, the SpG and ACE2 are collectively involved in disease establishment and 3CLpro, PLpro, RdRp involved in translation and replication lead to virus proliferation in the host cell. Therefore, these five proteins were considered as the therapeutic targets for the molecular docking with the selected 154 phytochemicals.

The dock score of the compounds against each protein are summarized in **Table S1**. The table of dock score of 154 phytochemicals against the five target proteins revealed that majority of the phytochemicals showed dock score higher than -6.5 Kcal/mol, and comparably higher dock score than the western drugs hydroxychloroquine and arbidol studied as a control. As the core part of all the compounds are similar, 20 compounds from each protein that showed the maximum dock score were selected for further screening (**Table S2**). Accordingly, total 47 compounds were considered for further *in silico* ADMET and drug-likeness study.

3.3. *In silico* ADMET and drug-likeness results

The 47 compounds selected based on their higher dock score were screened further for *in silico* ADMET and drug-likeness study. Considering the computational prediction and the

available experimental evidences on their pharmaceutical properties, the best 6 compounds for each protein target (i.e., total 15 phytochemicals) were selected for protein-ligand interaction study to identify the potential hits that bind at the catalytic sites of the respective protein (**Table 1**). These 15 compounds are obeying ADMET limitations and drug likeness LogP values. These compounds satisfied the limitations of lipophilicity, hydrophobicity and polarity. These compounds drug-likeness properties screened based on miLogP (molinspiration LogP) values and TPSA (Molecular polar surface area) [26]. This study helps in screening out the best compound with drug-likeness and polarity of compound permeable in biological system. The results of ADMET properties are given in the supplementary data (**Table S3**). ADMET results are interpreted based on marginal values compared with resultant value as high caco-2 permeability predicted value >0.90 , intestinal absorption less than 30% is considered as poorly absorbed, human VDss is low if it is below 0.71 L/kg and high value above 2.81L/kg, BBB permeability $\log BB > 0.3$ considered as it cross BBB and $\log BB < -1$ are poorly distributed. CNS permeability interpreted through $\log PS > -2$ penetrate CNS and $\log PS < -3$ as unable to penetrate. T. pyriformis toxicity predicted value > -0.5 ug/L considered as toxic and Minnow toxicity $\log LC50 < -0.3$ considered as high acute toxicity [27]. The most of the potent compounds finalised are found in the extracts of medicinal plants like neem, basil, licorice and citrus (**Table 1**).

Table 1. List of potent phytochemicals screened based on *in silico* ADMET, drug-likeness and published pharmaceutical data.

Compounds	Sources	Medicinal Properties	miLogP	TPSA	Ref
Corosolic acid	Lagerstroemia speciosa	Supress proliferation of cancer cells	5.87	77.75	28
Glycyrrhizic acid	Licorice	Treats liver diseases, Anti HIV-1, SARS-CoV	1.97	267.04	29,30
Maslinic acid	Olives	Anti-oxident, anti-inflammatory, weak inhibition to cytochrome P450	5.81	77.75	31
2-Hydroxysegenanolide	Fruits of Khaya senegalensis	Antifungal activity especially against <i>botrytis cinerea</i>	1.47	132.51	32

Oleanane	woody angiosperms	Antioxidant, anti-inflammatory, hepatoprotective, cardioprotective, antipruritic, spasmolytic, antiallergic, antimicrobial and antiviral effects and anti canceral especially breast cancer	8.86	0	33
7-Deacetyl-7-benzoylgedunin	Neem (Azadirachta indica)	Activity against HL60 leukemia cells	6.07	95.35	34
Epoxyazadiradione	Neem (Azadirachta indica)	Plasmodium falciparum plasmeprin I inhibitor	3.66	86.11	35
Limonoid	Citrus Fruits	Inhibit the HIV 1 replication in cellular systems	2.53	104.58	36
7-Deacetylgedunin	Neem (Azadirachta indica)	Antimalarial, anti-inflammatory	3.64	89.27	37
Oleanolic acid	Ocimum Sanctum (Basil)	Therapeutic potential for neurodegenerative diseases	6.72	57.53	38
Ursolic acid	Ocimum Sanctum (Basil)	Therapeutic potential for neurodegenerative diseases	6.79	57.53	39
Limonin17 beta-Dglucopyranoside	Citrus Fruits	Inhibit colon adenocarcinoma cell proliferation through apoptosis	-0.29	214.96	40
Azadiradionolide	Neem (Azadirachta indica)	Apoptosis inducing activity	2.85	86.75	41
Gedunin	Neem (Azadirachta indica)	Antiplasmodial	4.34	95.35	42
Obacunone	Citrus Fruits	Represses salmonella pathogenicity and also inhibits human colon cancer	3.8	95.35	43

3.4. Protein-ligand interaction study

3.4.1. Screening of inhibitors for main protease

The main protease 3CLpro is a cysteine protease containing three domains, i.e., domains I (8-101 residues) and II (102-184 residues) with antiparallel β -barrel structure and the domain III (201-303 residues) with five α -helices is linked to the domain II by a long loop (185-200 residues) [44]. The catalytic dyad residues Cys145 and His41 are involved in substrate cleavage and present in the cleft between domain I and II. The enzyme active site consists of 6 subunits (S1-S6), the active site residues are 140-145 and 163-166 amino acids in the domain II. The best

6 compounds finalised based on the dock score with 3CLpro followed by *in silico* ADMET and drug-likeness are summarized in Table 2 along with the important molecular interactions.

The main protease complex with the phytochemicals 7-deacetyl-7-benzoylgedunin is showing binding affinity at the catalytic dyad (**Fig. 1** and **Fig. S1**). Catalytic dyad pocket shows ligand binds to Cys145 forming π -alkyl interaction and His41 forming π -cation interactions [44]. The 7-deacetyl-7-benzoylgedunin had shown dock score -9.1kcal/mol at the active site of 3CLpro long loop region of domain II (1)(2). The interaction study of 7-deacetyl-7-benzoylgedunin results in C-H bond interaction to Thr26 and showing unfavourable bond to Gln189 and His164. The closest VDW forces with the residues Glu166, Arg188, Leu167, Gln192, Thr190, Met49, Gly143, Thr25 and Asn142 of the domain II antiparallel β -barrel structure. The protein structural simulation generated RMSF graph showing protein residues fluctuation and aggregation (**Fig. S2**). The fluctuated residues showing the hydrophobic cavities where substrate binding, catalytic functions took place. For 3CLpro simulation, some of the residues fluctuation impact of chain A (5-16, 46-56, 136-151, 165-178, 181-196, 241-260, 271-286) and fluctuation impact showing ligand interactions at these residues.

The phytochemicals glycyrrhizic acid showing highest dock score -9.3kcal/mol bind at the C terminal residues that are Asn274, Gly275, Leu286, Leu287, Asp289, Glu288, Arg131, Glu290, Asn238, Thr198, Tyr239, Leu272, Gln273 showing VDW forces and Tyr237, Lys137, Thr199 forming H bonding at the hydrophobic site containing largest ligand-binding cavity but the activity is unknown. Ursolic acid and oleanolic acid isolated from holy basil leaves are also effectively targeting the Mpro active sites forming hydrogen bonds to Lys137, Leu272 and closest non-covalent interactions with Thr199, Arg131, Leu287 residues with maximum binding energy -8.9 kcal/mol. Similarly, the interaction sites of other phytochemicals limonin and

obacunone binding at C terminal hydrophobic pocket are also summarized and compared (Table 2).

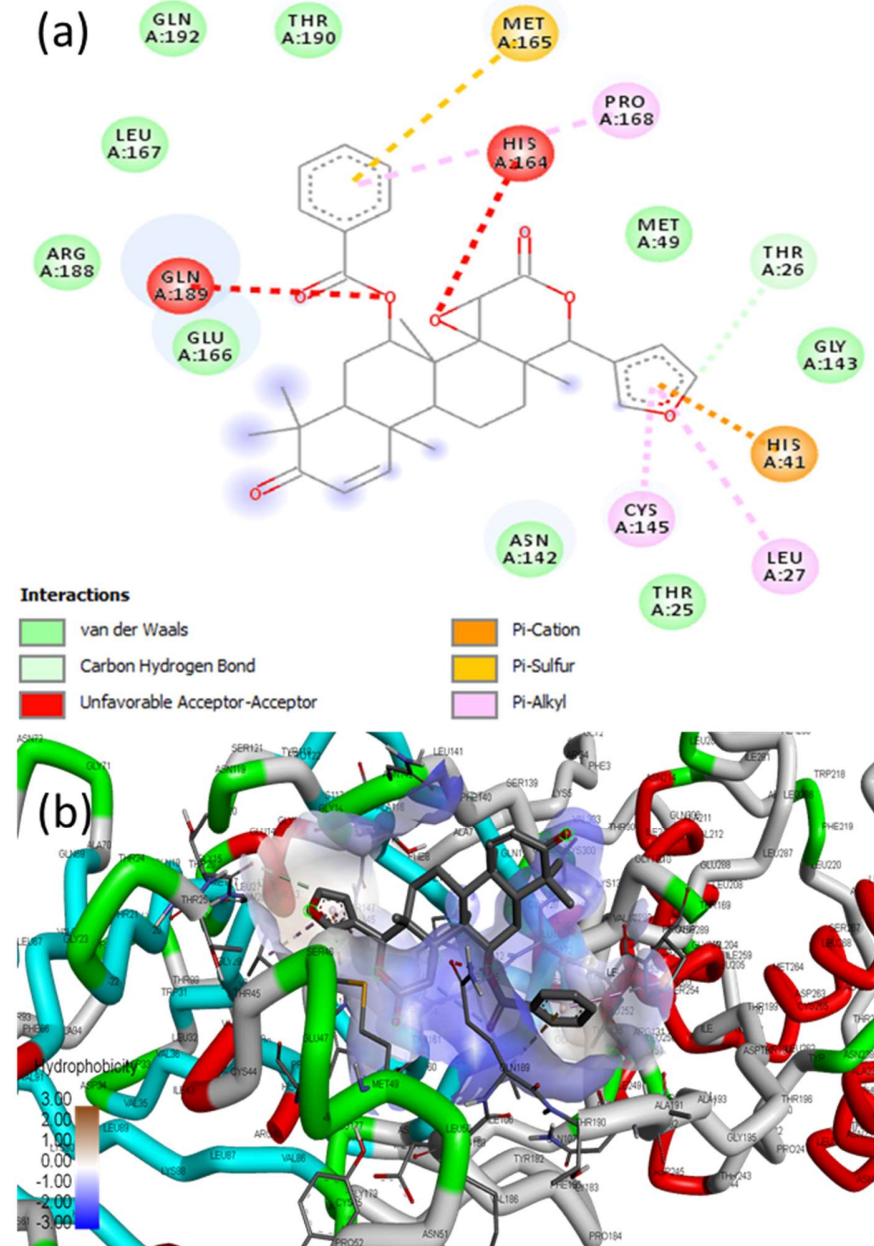


Fig. 1. (a) 2D animated pose between 7-deacetyl-7-benzoylgedunin and 3CLpro showing various non-covalent interactions, (b) 3D representation showing the position of 7-deacetyl-7-benzoylgedunin within the hydrophobic cavity of 3CLpro.

Table 2. Screened phytochemicals used for protein-ligand interaction study against the main protease 3CLpro.

Phytochemicals	B.E. (Kcal/mole)	Molecular interactions
7-deacetyl-7-benzoylgedinin	-9.1	A: C : Thr26, H : Glu166, VDW : Arg188, Leu167, Gln192, Thr190, Met49, Gly143, Thr25, Asn142, π - π : A: Pro168, Leu27, Cys145, Cationic : His41, Met165
Glycyrrhizic acid	-9.3	A: H : Tyr237, Lys137, Thr199, C : Asp197 VDW : Asn274, Gly275, Leu286, Leu287, Asp289, Glu288, Arg131, Glu290, Asn238, Thr198, Tyr239, Leu272, Gln273
Limonin	-8.7	A: H : Thr199, C : Leu287 VDW : Leu272, Tyr239, Tyr237, Asn238, Gly275, Met276, Leu286, Leu271, Lys137, Cationic : A: Arg131, Anionic : A: Asp289
Oleanolic acid	-8.9	A: H : Lys137, Leu271, Leu272 VDW : Gln273, Gly275, Met276, Leu287, Tyr239, Leu286, Thr199, Arg131, Asp197, Asn238, Tyr237
Ursolic acid	-8.9	A: H : Lys137, Leu272, VDW : Asp197, Thr198, Arg131, Asp289, Thr199, Leu286, Tyr239, Leu287, Met276, Gly275, Leu271, Gln273, Tyr237
Obacunone	-8.7	A: H - A: Met276, C : Gly275, π - π - Leu286 VDW : Tyr237, Tyr239, Thr199, Ala285, Leu271, Leu272, Leu287, Asp289, Glu288.

3.4.2. Screening of inhibitors for PLpro

PLpro consists of four domains such as thumb, finger, palm and ubiquitin like domain. The active site located in between the thumb and palm domains [45]. The subunits consist of catalytic triad (Cys112, His273, Asp287), where the active site is located. PLpro NSP3 domain contains S2/S4 inhibitor binding sites. Therefore, the molecular screening of phytochemicals that docked at specific residues of S2/S4 site could inhibit the activity of PLpro [45]. The dock score along with the molecular interactions of the best 6 phytochemicals are summarized in Table 3.

The protein-ligand interaction study revealed that the epoxyazadiradione binds exactly at the S2 active site of PLpro with the binding energy -8.4 kcal/mol. At the active site, the ligand targeted residues Gly164 and Tyr274 are forming H bond. Residues Pro248 and Pro249 forming π -alkyl interaction. Residues Leu163, Gln270, Tyr269, Met209, Thr302, Asp165, Tyr265, Cys271 and Gly272 are showing VDW interactions (**Fig. 2** and **Fig. S3**). Epoxyazadiradione

binding at the pocket of catalytic triad (Cys112, His273, Asp287) residues can hindrance the enzymatic activity of PLpro [46,47]. Further, the MD simulations generated RMSF plot of PLpro showing available contacts to substrate at chain B (5-10, 170-185, 265-270) residues (**Fig. S4**).

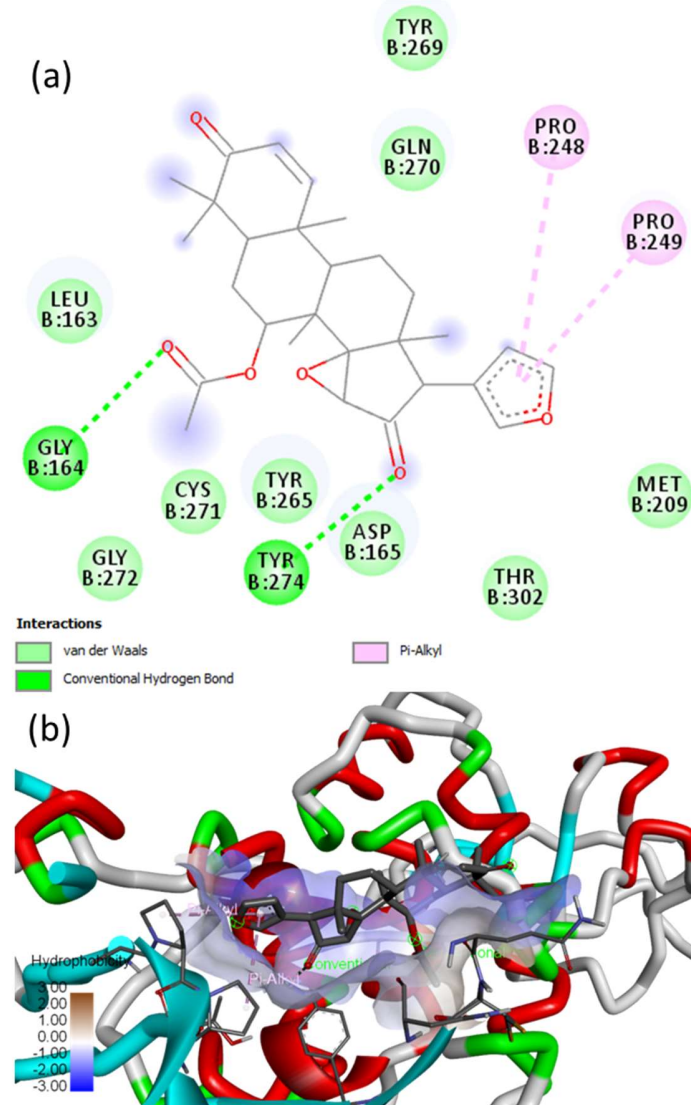


Fig. 2. (a) 2D animated pose between epoxyazadiradione and PLpro showing various non-covalent interactions, (b) 3D representation showing the position of epoxyazadiradione within the hydrophobic cavity of PLpro.

The protein-ligand interaction study of other best dock score phytochemicals revealed that the binding site are not at the catalytic triad. The NSP3 domain S4 subunit active site docked

with 7-deacetylgedunin showing -8.2 kcal/mol binding energy. Residues like Gln270, Lys158 showing H bond and VDW forces observed at the residues Thr302, Pro249, Tyr265, Tyr269, Cys271, Asn268, Leu163, Glu162, Asp165 and Tyr274. One of the limonoid 7-deacetyl-7-benzoylgedunin, which is a potent inhibitor of Mpro active site showing the maximum affinity to PLpro hydrophobic site but the activity of the site is not reported. This site forming H bond to Arg141, Gln134 and Glu125, C bond and VDW forces to Leu124, Gln122, Gln123, Val126, Lys127 and Glu135.

Table 3. Screened phytochemicals used for protein-ligand interaction study against the PLpro.

Phytochemicals	B.E. (Kcal/mole)	Molecular interactions
Epoxyazadiradione	-8.4	B:H-Gly164,Tyr274, VDW :Leu163,Gln270,Tyr269,Met209, Thr302,Asp165,Tyr265, Cys271,Gly272, π-π : Pro248,Pro249
Glycyrrhizic acid	-9.0	B: H : Leu76, Thr7, Asp77, Arg83, Asn157, Asn129, ASn178, B:His74, VDW : Phe80,Ala154,Gln175,His172,His176,Glu180,Phe70
7-Deacetyl-7-benzoylgedunin	-8.3	B: H - B: Arg141,Gln134, C-H - B: Glu125 VDW : Leu124,Gln122,Gln123,Val126,Lys127,Glu135 π-π - B: Tyr138
Limonin	-8.3	B: H :Arg167,Gln175, VDW :Leu200,Gln233,Arg184,Tyr208,Leu186, Met209, Met207,Thr171. π-π - B: Val203, Anionic - B: Glu204
7-Deacetylgedunin	-8.2	B: H :Gln270,Lys158, VDW :Thr302,Pro249,Tyr265,Tyr269, Cys271,Asn268,Leu163, Glu162,Asp165,Tyr274
Obacunone	-8.2	B: H :Met209,Arg167, VDW :Leu200,Glu204,Gln175, Met207,Tyr208, Arg184,Leu186, Gln233

3.4.3. Screening of inhibitors for RdRp (NSP12 domain)

RdRp, the non-structural protein NSP12 is a replication tools plays a major role in transcription cycle of virus with the help of cofactors (NSP7, NSP8). So the primary target of the RdRp is NSP12, where the active sites are located. RdRp consists of NSP12-NSP7-NSP8 domains, where the active site is in between the NiRAN domain β-hairpin [49]. There are more than 80 phytochemicals showed activity against RdRp functional sites. We selected 6 compounds based on the higher dock scores, known medicinal properties, *in silico* ADMET and drug likeness predictions. The interaction details of the top 6 ligands were given in the Table 4.

Limonin (furanolactones), a potent phytochemicals docked at the active site between NSP12-NSP7 residues. Limonin is encapsulated within the receptor cavity showing hydrophobic surface and maximum binding energy -9.2kcal/mol (**Fig. 3** and **Fig. S5**). RdRp substrate-binding site interacting with limonin formed H bond to Ser709, Lys714, Asp711, Thr710 maintaining strong affinity and that includes non-covalent VDW forces between ligand and Gln773, Gly774, Asn781, Lys780, Ser784, His133, Lys47, Asn138, Tyr129, Asp135, Thr710, Tyr32 in the active pocket. RdRp structural contacts in chain A: 31-45, 255-285, 419-459, 909, B chain: 103 and 148-188 residues showing hydrophobic cavities, substrate binding sites involved in replication process and those are resembling in the RMSF plot (**Fig. S6**).

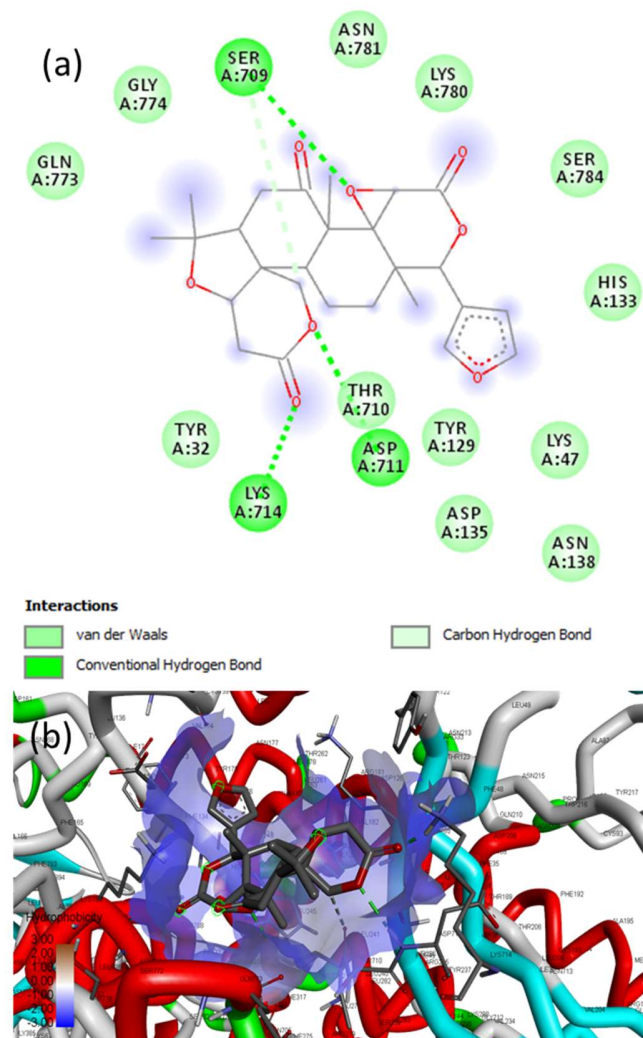


Fig. 3. (a) 2D animated pose between limonin and RdRp showing various non-covalent interactions, (b) 3D representation showing the position of limonin within the hydrophobic cavity of RdRp.

Glycyrrhizic acid is also encapsulated in the receptor cavity with maximum binding energy -9.9kcal/mol and the site located between NiRAN domain and β -hairpin structure that polymerize 3' end [49]. Glycyrrhizic acid could cause interference to β -hairpin polymerize activity due to its binding affinity at the active site residues Tyr129, Ser772, Asn781, Asn138 and closest non-covalent interactions to Gln773, Lys714, Tyr32, Asp711, Ser784, Lys780, Gly774, Ser778, Ala706, Thr710, Asp135, His133, Cys139, Lys47. Other limonoids showing binding affinity to RdRp hydrophobic cavities are 7-deacetyl-7-benzoylgedunin, 7-deacetylgedunin, limonin-17beta-D-glucopyranoside and obacunone (**Table 4**).

Table 4. Screened phytochemicals used for protein-ligand interaction study against the RdRp.

Phytochemicals	B.E. (Kcal/mole)	Molecular interactions
Limonin	-9.2	A: H : Ser709, Lys714, Asp711, Thr710 VDW : Gln773, Gly774, Asn781, Lys780, Ser784, His133, Lys47, Asn138, Tyr129, Asp135, Thr710, Tyr32
Glycyrrhizinic acid	-9.9	A: H : Ser772, Tyr129, Asn781, Asn138 VDW : Gln773, Lys714, Tyr32, Asp711, Ser784, Lys780, Gly774, Ser778, Ala706, Thr710, Asp135, His133, Cys139, Lys47
7-deacetyl-7-benzoylgedunin	-9.7	A: H : Ser255 VDW : Phe321, Pro323, Arg349, Pro677, THr246, Thr319, Thr252, Val320. π-π : Pro461, Tyr265, Arg249
7-deacetylgedunin	-8.8	A: H : Lys780, Ser784, Asn781, C-H : Ala706, Gly774 Asn138, Asp135, His133, Tyr129, Ser709, Ala706, Thr710, Lys47, Tyr32. π-π : Ala706
Limonin17bDglucopyranoside	-8.9	A : H - His133, Ser784, Lys780, Ala706, Asp711 C : Thr710, Gly774 VDW - Asn138, Phe134, Ser709, Lys714, Ser772, Gln773, Asp135
Obacunone	-8.7	A: C : Thr319, Thr252, VDW : Lys267, Tyr265, Arg249, Leu251, Ser255, Val320, Ile266, Phe321, Trp268, Pro323, Pro322

3.4.4. Screening of inhibitors for SGp-RBD

The spike proteins determine the virion-host tropism that includes the entry of the virions into host cells, and their interactions with human ACE2. It constitutes the target prominent that plays a key role in the development of the procatylitics and therapeutics [50]. Two states in receptor binding domains (RBD) namely buried (lying state) or exposed (standing state) were observed in the recent reports coming up with structures of the different CoV's that are inherently flexible with the RBD's [50]. Due to its structural importance, we focused on SGp-RBD inhibition study by screening 157 phytochemicals through molecular docking and binding confirmations at 3 active sites that could inhibit the SGp and hinder SGp-ACE2 complex formation. Spike glycoprotein RDB contains 333-527 residues where the active sites are located [51]. The molecular interactions between the best 6 phytochemicals with the SGp sites are shown in Table 5.

Maslinic acid binding at the RBD where the initial contact was made towards ACE2. Maslinic acid with binding energy -9.3kcal/mol, forming a complex at C chain with a possible interactions to site-1: H bond to Arg441, non-covalent (VDW) interactions to Ser456, Leu443, Pro459, Iy464, Lys465 and (Alkyl- π -alkyl) interactions to His445, Phe460, Arg444, Pro477, Pro466 (**Fig. 4** and **Fig. S7**). It is also forming a complex at E chain site-2, H bond to Asp480, Tyr440 an unfavourable donor-donor interaction, Alkyl- π -alkyl to Tyr484, Tyr491, Lys390 and VDW to Tyr436, Gly482, Thr486, Thr487, Asn479, Tyr481 (**Fig. S8**). In site-3, the maslinic acid binding to an active cavity at chain E residues Ser358, Ala331 forming H bond and non-covalent VDW interactions to Phe360, Asn427, Thr332, Asn424, Asn357, Thr359, Ile428, Trp423, Phe329, Tyr356, Thr425, Arg495, Asn330 (**Fig. S9**). Maslinic acid collectively forms hydrophobic interactions at site-1, site-2 and site-3 that could hinder the SpG-RBD complex with ACE2 host receptor. MD simulations of SpG-RBD complex generated the RMSF plot detailing

contact sites are showing the fluctuations in chain C: 432-438, 352-368, and 456-480, residues of receptor binding sites (**Fig. S10**).

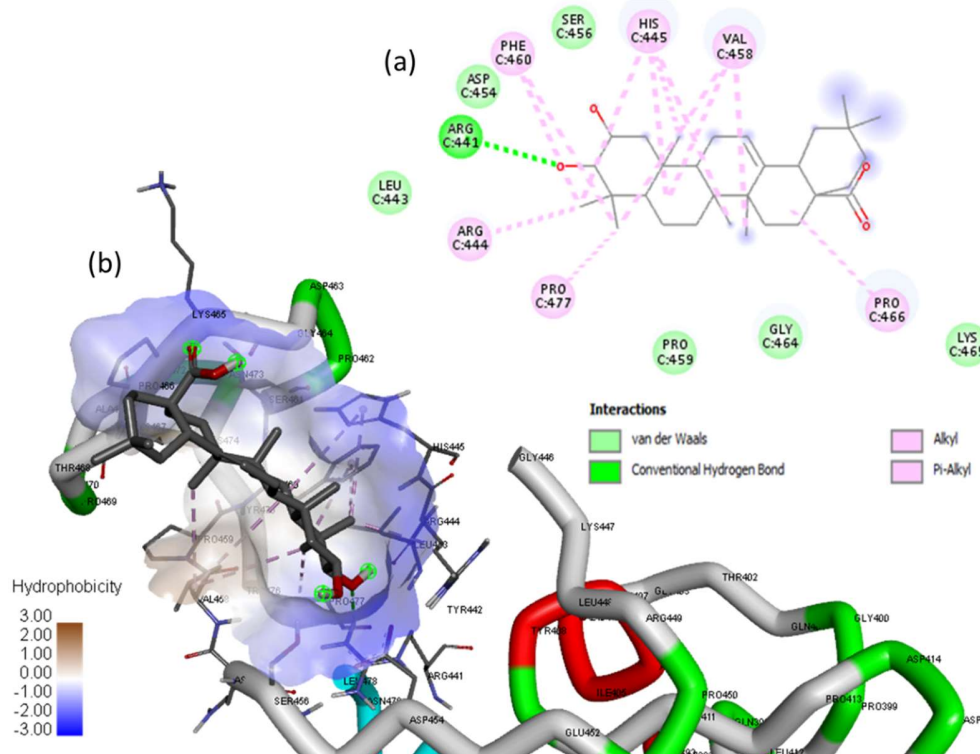


Fig. 4. (a) 2D animated pose between maslinic acid and SGp-RBD at site-1 showing various non-covalent interactions, (b) the corresponding 3D representation showing the position of maslinic acid within the hydrophobic cavity of SGp-RBD.

The phytochemical corosolic acid showed maximum binding affinity (-9.4 kcal/mol) to site-3 of RBD residues Asn330, Phe334, Ala331, Phe329, Arg495, Trp423, Thr425, Thr359, Ser358, Phe360, Asn424, Asn427, Tyr356, Ile428, Thr332. Glycyrrhizic acid encapsulated at the active site-3 with B.E -9.3kcal/mol having H bond to Phe360, Arg426, Asn427, Trp423, Thr333 and non-covalent VDW to Tyr356, Asn357, Ser358, Phe361, Ser362, Ile489, Gln492, Asn424, Thr359, Thr425, Arg495, Ile428, Asn330, Ala332 residues. 2-Hydroxysemenegolide and Gedunin binding to active sites of chain C residues with B.E -9.2 and -8.2kcal/mol respectively

to Trp423 and Gly368 by H bond. Oleanane binding to E chain active sites with closest non-covalent VDW interaction to Thr332, Ala331, Tyr356 residues.

Table 5. Screen phytochemicals used for protein-ligand interaction study against the SGp-RBD.

Phytochemicals	B.E. (Kcal/mole)	Molecular interactions
Maslinic acid	-9.3	C: H- Arg441 VDW -Leu443, Asp454, Ser456, Pro459, Gly464, Lys465 π-π :Phe460, His445, Arg444, Pro477, Pro466
Corosolic acid	-9.4	E: VDW -Asn330,Phe334,Ala331,Phe329,Arg495,Trp423, Thr425, Thr359,Ser358,Phe360,Asn424,Asn427,Tyr356,Ile428,Thr332
Glycyrrhizic acid	-9.3	E: H: Phe360, Arg426,Asn427,Trp423, Thr333, C:Ser363 VDW :Tyr356,Asn357,Ser358,Phe361,Ser362,Ile489,Gln492,Asn 424,Thr359,Thr425,Arg495,Ile428,Asn330,Ala332
2-Hydroxyseneganolide	-9.2	C:H:Trp423, VDW :Asn330,Phe329,Thr359,Thr425,Asn427, Asn424,Ser358, Tyr356,Asn357,Thr332,Ala331,Arg495
Oleanane	-9.0	E: VDW :Thr332,Ala331,Tyr356,Asn330,Phe329,Arg495, Trp423,Thr359,Asn424,Phe360,Ser358,Asn427,Thr425
Gedunin	-8.2	C: H:Gly368, VDW: Asp415, Asp414, π-π :Pro399, Lys365, Ala398

3.4.5. Screening of inhibitors for ACE2

ACE2 plays a key role in cardio renal disease and acts as a human host receptor for the SARS and helps in viral-host interactions [52]. ACE2, a human viral receptor binds to SGp RBD at a specific site that establishes the primary contact for host-pathogen interaction [53]. The active site residues of ACE 2 were studied by using site-directed mutagenesis and it was found that Arg273 plays a critical role in substrate binding, whereas the consequence of its replacement results in the abolishment of the enzyme activity. Also, His 345 plays an important role as a hydrogen bond donor/acceptor to form the tetrahedral peptide intermediate [53]. From the computational approaches, the best 6 phytochemicals showing higher binding affinity at hydrophobic sites along with the molecular interactions are summarized in Table 6.

Glycyrrhizic acid, the triterpenoid is showing better binding affinity (-10.3 kcal/mol) to RBD and ACE2 active sites. The receptor binding cavity interacts with glycyrrhizic acid through

Tyr202, Gln102, Ser106, Ser70 H-bonds, and Asp350, Trp349, Phe40, Tyr385, Arg393, Asn394, Trp69, Phe390, Leu391, Ala99, Leu73, Leu100, Lys74, Ser77, Asn103, Gly104 non-covalent VDW forces (**Fig. 5** and **Fig. S11**). Glycyrrhizic acid could potentially interfere with the SGp-RBD-ACE2 complex formation. MD simulations of ACE2 complex with glycyrrhizic acid showing multiple contact sites. Some of the sites states SGp receptor forming a complex to ACE2 in host cells in receptor chain B: 51-81, 141, 201-231, 261, 321-351, 531-561, 591-651 residues (**Fig. S12**). Out of these residues, the SpG-ACE2 initial contact take place in Q24, M82, L79, K31, H34, E37, G354, Q325, D38, N330, E 329, Q42, L45 residues.

The phytochemicals ursolic acid, maslinic acid and obacunone showed comparable binding affinity to the ACE2. In case of ursolic acid, the hydrophobic cavity residues exhibit H bond to His493, and VDW forces to Lys475, Glu479, Arg482, Trp478, Tyr613, Glu489, Met474, Pro492, Glu495, Ala673, Asn674, Asp494 and Leu675 along with a C bond to Pro492. The interactions of other phytochemicals are summarized in Table 6.

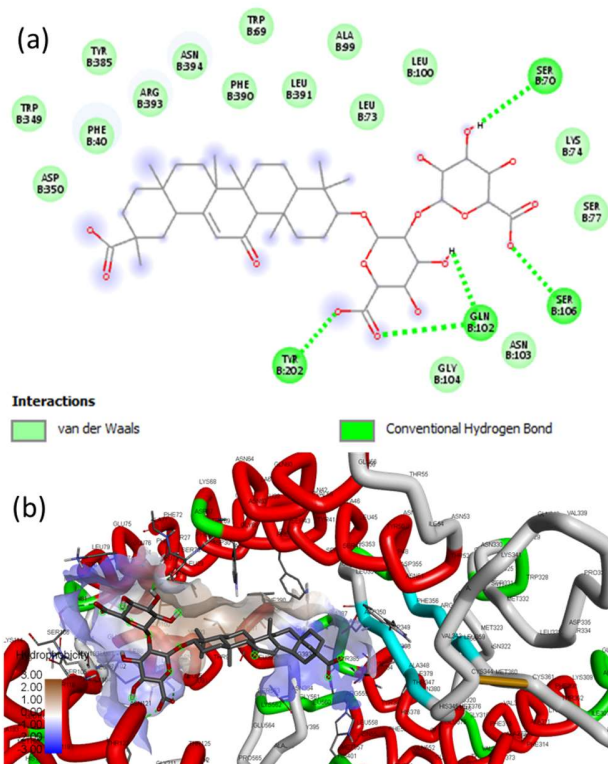


Fig. 5. (a) 2D animated pose between glycyrrhizic acid and ACE2 showing various non-covalent interactions, (b) 3D representation showing the position of glycyrrhizic acid within the hydrophobic cavity of ACE2.

Table 6. Screen phytochemicals used for protein-ligand interaction study against the ACE2.

Phytochemicals	B.E. (Kcal/mole)	Molecular interactions
Glycyrrhizinic acid	-10.3	B: H: Tyr202, Gln102, Ser106, Ser70 VDW: Asp350, Trp349, Phe40, Tyr385, Arg393, Asn394, Trp69, Phe390, Leu391, Ala99, Leu73, Leu100, Lys74, Ser77, Asn103, Gly104
Ursolic acid	-10.2	B: H: B: His493, C: B: Pro492 VDW: Lys475, Glu479, Arg482, Trp478, Tyr613, Glu489, Met474, Pro492, Glu495, Ala673, Asn674, Asp494, Leu675
Maslinic acid	-10.2	B: H: Asn674, Glu495, C: Asn674, Glu489, Asp494 Arg482, Ser611, Tyr613, Trp478, Ala673, Pro492, His493, Val672, Met640, Leu675, Lys475, Glu479
Obacunone	-10.2	B: VDW: Arg482, Glu479, Lys475, Asp471, Leu675, Asp494, Ala673, Pro492, Asn674, His493, Glu489, Tyr613
Azadiradionolide	-9.8	B: VDW: Arg644, Val672, Leu675, Ala673, Asn674, Trp478, Lys475, His493, Met474, Asp494, Glu495, Thr496, Met640, Asp637, Arg644
Gedunin	-9.9	B: Trp478, Glu479, Asn674, Lys475, Lys676, Glu495, Leu675, Asp494, Met640, His493, Pro492, Ala673, Glu489, Tyr613, Arg482, π-π - B: Val672

4. Conclusions

In summary, the screening of 154 phytochemicals from limonoids and triterpenoids by molecular docking, *in silico* ADMET and drug likeness with five protein targets (3CLpro, PLpro, RdRp, SpG, ACE2) resulted 15 effective phytochemicals, from which best six phytochemicals were proposed as potential hits against the SARS-CoV-2. Among the six, the two neem isolates 7-deacetyl-7-benzoylguedunin posing binding energy -9.1kcal/mol to cleave substrate binding site catalytic dyad residues (Cys145 and His41) of 3CLpro, a potential lead to inhibit proteases involved in the process of proteolysis of viral polyprotein into functional units and Epoxyazadiradione an active lead inhibiting the PLpro S2 subunit with -8.4kcal/mol binding energy to pocket consisting of Catalytic Triad (Cys112, His273, Asp287). A citrus fruit seed isolate limonin inhibiting the RdRp substrate binding site at NSP12-NSP7 residues with the B.E -9.2kcal/mol that inhibits the polymerase activity due to hindrance in NiRAM replication fork. Neem and Citrus fruits isolates potentially blocks the SARS-CoV-2 translation and replication functions. Maslinic acid, corosolic acid and 2-hydroxyseneganolide are potent inhibitors of SGp-RBD active sites that hinder to dock hACE2 receptor. Glycyrrhizic acid including ursolic acid could potentially interfere with the ACE2-SGp RBD complex with binding energy - 10.3kcal/mol. Olives, holy basil and licorice triterpenoids potentially obstruct SGp and ACE2 receptors disease establishment. Therefore, the computational predictions along with the reported pharmacological properties postulated that the limonoids and triterpenoids are potential against SARS-CoV-2 target proteins. The outcomes will be useful in formulating therapeutic strategies using the traditional medicines as well as the potential hits can be used for lead optimization for drugs discovery for SARS-CoV-2.

References

1. <https://www.who.int/emergencies/diseases/novel-coronavirus-2019/situation-reports>.
2. https://en.wikipedia.org/wiki/Severe_acute_respiratory_syndrome_coronavirus_2.
3. Zhou, Y., et al., 2020. Network-based drug repurposing for novel coronavirus 2019-nCoV/SARS-CoV-2. *Cell Discovery*, 6(1).
4. Singh, A., et al., 2020. Chloroquine and hydroxychloroquine in the treatment of COVID-19 with or without diabetes: A systematic search and a narrative review with a special reference to India and other developing countries. *Diabetes & Metabolic Syndrome: Clinical Research & Reviews*, 14(3), pp.241-246.
5. Zhu, Z., et al., 2020. Arbidol monotherapy is superior to lopinavir/ritonavir in treating COVID-19. *Journal of Infection*,
6. Choy, K., et al., 2020. Remdesivir, lopinavir, emetine, and homoharringtonine inhibit SARS-CoV-2 replication in vitro. *Antiviral Research*, 178, p.104786.
7. Dong, L., et al., 2020. Discovering drugs to treat coronavirus disease 2019 (COVID-19). *Drug Discoveries & Therapeutics*, 14(1), pp.58-60.
8. McKee,D., et al., 2020. Candidate drugs against SARS-CoV-2 and COVID-19. *Pharmacological Research*, 157, p.104859.
9. Yang, Y., et al., 2020. Traditional Chinese Medicine in the Treatment of Patients Infected with 2019-New Coronavirus (SARS-CoV-2): A Review and Perspective. *International Journal of Biological Sciences*, 16(10), pp.1708-1717.
10. Liu, M., et al., 2020. Efficacy and Safety of Integrated Traditional Chinese and Western Medicine for Corona Virus Disease 2019 (COVID-19): a systematic review and meta-analysis. *Pharmacological Research*, p.104896.
11. Ho, L., et al., 2020. Highlights of traditional Chinese medicine frontline expert advice in the China national guideline for COVID-19. *European Journal of Integrative Medicine*, 36, p.101116.
12. Ryu, Y., et al., 2010. SARS-CoV 3CLpro inhibitory effects of quinone-methide triterpenes from Tripterygium regelii. *Bioorganic & Medicinal Chemistry Letters*, 20(6), pp.1873-1876.
13. Pillaiyar, T., et al., Manickam, M., Namasivayam, V., Hayashi, Y. and Jung, S., 2016. An Overview of Severe Acute Respiratory Syndrome–Coronavirus (SARS-CoV) 3CL Protease

Inhibitors: Peptidomimetics and Small Molecule Chemotherapy. *Journal of Medicinal Chemistry*, 59(14), pp.6595-6628.

14. Chang., et al., 2012, 'Anti-human coronavirus (anti-HCoV) triterpenoids from the leaves of *Euphorbia neriifolia*', *Natural product communications*, vol. 7, no. 11, pp. 1415-1417.
15. Fiore, C., et al., 2008. Antiviral effects of *Glycyrrhiza* species. *Phytotherapy Research*, 22(2), pp.141-148.
16. Vardhan, S., et al., 2020. Searching inhibitors for three important proteins of COVID-19 through molecular docking studies, arXiv:2004.08095.
17. Rezac, J., et al., 2009. Semiempirical Quantum Chemical PM6 Method Augmented by Dispersion and H-Bonding Correction Terms Reliably Describes Various Types of Noncovalent Complexes. *Journal of Chemical Theory and Computation*, 5(7), pp.1749-1760.
18. Trott, O., et al., 2009. AutoDock Vina: Improving the speed and accuracy of docking with a new scoring function, efficient optimization, and multithreading. *Journal of Computational Chemistry*, pp. 455-461.
19. Jamroz, M., et al., 2014. CABS-flex predictions of protein flexibility compared with NMR ensembles. *Bioinformatics*, 30(15), pp.2150-2154.
20. <http://biosig.unimelb.edu.au/pkcsdm/>.
21. <https://www.sciencedirect.com/topics/immunology-and-microbiology/lipophilicity>.
22. Yuan, Y., et al., 2017. Cryo-EM structures of MERS-CoV and SARS-CoV spike glycoproteins reveal the dynamic receptor binding domains. *Nature Communications*, 8(1), p. 15092.
23. Guy, J., et al., 2005. Identification of critical active-site residues in angiotensin-converting enzyme-2 (ACE2) by site-directed mutagenesis. *FEBS Journal*, 272(14), pp.3512-3520.

24. Liu, C., et al., 2020. Research and Development on Therapeutic Agents and Vaccines for COVID-19 and Related Human Coronavirus Diseases. *ACS Central Science*, 6(3), pp.315-331.

25. Kilianski, A., et al., 2013. Assessing Activity and Inhibition of Middle East Respiratory Syndrome Coronavirus Papain-Like and 3C-Like Proteases Using Luciferase-Based Biosensors. *Journal of Virology*, 87(21), pp.11955-11962.

26. <http://www.molinspiration.com/cgi-bin/properties>.

27. Pires, D., et al., 2015. pkCSM: Predicting Small-Molecule Pharmacokinetic and Toxicity Properties Using Graph-Based Signatures. *Journal of Medicinal Chemistry*, 58(9), pp.4066-4072.

28. Li, J., et al., 2014. Glycyrrhizic Acid in the Treatment of Liver Diseases: Literature Review. *BioMed Research International*, 2014, pp.1-15.

29. Yap, W., et al., 2015. Mechanistic Perspectives of Maslinic Acid in Targeting Inflammation. *Biochemistry Research International*, 2015, pp.1-9.

30. Graebin, C., et al., 2010. Glycyrrhizin and glycyrrhetic acid: scaffolds to promising new pharmacologically active compounds. *Journal of the Brazilian Chemical Society*, 21(9), pp.1595-1615.

31. Abdelgaleil., S.A., et al., 2004. Antifungal limonoids from the fruits of *Khaya senegalensis*. *Fitoterapia*, 75(6), pp.566-572.

32. Parikh., N.R., et al., 2014. Oleanane triterpenoids in the prevention and therapy of breast cancer: current evidence and future perspectives. *Phytochemistry Reviews*, 13(4), pp.793-810.

33. Takagi., M., et al., 2014. Cytotoxic and Melanogenesis-Inhibitory Activities of Limonoids from the Leaves of *Azadirachta indica* (Neem). *Chemistry & Biodiversity*, 11(3), pp.451-468.

34. Kikuchi, T., et al., 2011. Cytotoxic and Apoptosis-Inducing Activities of Limonoids from the Seeds of *Azadirachta indica* (Neem). *Journal of Natural Products*, 74(4), pp.866-870.

35. Thillainayagam, M., et al., 2018. Insights on inhibition of *Plasmodium falciparum* plasmepsin I by novel epoxyazadiradione derivatives – molecular docking and comparative molecular field analysis. *Journal of Biomolecular Structure and Dynamics*, 37(12), pp.3168-3182.

36. Battinelli, L., et al., 2003. Effect of Limonin and Nomilin on HIV-1 Replication on Infected Human Mononuclear Cells. *Planta Medica*, 69(10), pp.910-913.

37. Miranda Júnior, R., et al., 2012. Antiplasmodial activity of the andiroba (*Carapa guianensis* Aubl., Meliaceae) oil and its limonoid-rich fraction. *Journal of Ethnopharmacology*, 142(3), pp.679-683.

38. Laura, C., et al., 2015. Oleanolic acid: a promising neuroprotective agent for cerebral ischemia. *Neural Regeneration Research*, 10(4), p.540.

39. Ramos-Hryb., A.B., et al., 2017. Therapeutic Potential of Ursolic Acid to Manage Neurodegenerative and Psychiatric Diseases. *CNS Drugs*, 31(12), pp.1029-1041.

40. Murthy, K.N.C., et al., 2011. Citrus Limonin and Its Glucoside Inhibit Colon Adenocarcinoma Cell Proliferation through Apoptosis. *Journal of Agricultural and Food Chemistry*, 59(6), pp.2314-2323.

41. Kingston, D., et al., 2011. Modern Natural Products Drug Discovery and Its Relevance to Biodiversity Conservation. *Journal of Natural Products*, 74(3), pp.496-511.

42. Chianese, G., et al., 2010. Antiplasmodial Triterpenoids from the Fruits of Neem, *Azadirachta indica*. *Journal of Natural Products*, 73(8), pp.1448-1452.

43. Murthy, K.N.C., et al., 2011. Obacunone and obacunone glucoside inhibit human colon cancer (SW480) cells by the induction of apoptosis. *Food and Chemical Toxicology*, 49(7), pp.1616-1625.

44. Jin, Z., et al., 2020. Structure of Mpro from COVID-19 virus and discovery of its inhibitors. *Nature*, DOI: 10.1038/s41586-020-2223-y.

45. Baez-Santos, Y., et al., 2014. Catalytic Function and Substrate Specificity of the Papain-Like Protease Domain of nsp3 from the Middle East Respiratory Syndrome Coronavirus. *Journal of Virology*, 88(21), pp.12511-12527.

46. Báez-Santos., Y.M., et al., 2015. The SARS-coronavirus papain-like protease: Structure, function and inhibition by designed antiviral compounds. *Antiviral Research*, 115, pp.21-38.

47. Barreto, N., et al., 2005. The Papain-Like Protease of Severe Acute Respiratory Syndrome Coronavirus Has Deubiquitinating Activity. *Journal of Virology*, 79(24), pp.15189-15198.

48. Kirchdoerfer, R., et al., 2019. Structure of the SARS-CoV nsp12 polymerase bound to nsp7 and nsp8 co-factors. *Nature Communications*, 10(1).

49. Gao, Y., et al., 2020. Structure of the RNA-dependent RNA polymerase from COVID-19 virus. *Science*, p.eabb7498.

50. Letko, M., et al., 2020. Functional assessment of cell entry and receptor usage for SARS-CoV-2 and other lineage B betacoronaviruses. *Nature Microbiology*, 5(4), pp.562-569.

51. Yuan, M., et al., 2020. A highly conserved cryptic epitope in the receptor binding domains of SARS-CoV-2 and SARS-CoV. *Science*, 368(6491), pp.630-633.

52. Rodell, C., et al., 2020. An ACE therapy for COVID-19. *Science Translational Medicine*, 12(541), p.eabb5676.

53. Wu, K., et al., 2009. Crystal structure of NL63 respiratory coronavirus receptor-binding domain complexed with its human receptor. *Proceedings of the National Academy of Sciences*, 106(47), pp.19970-19974.